

# Excitation Induced Dephasing in Semiconductor Quantum Dots

H. C. Schneider

*Physics Department, Kaiserslautern University of Technology,  
P. O. Box 3049, 67653 Kaiserslautern, Germany*

W. W. Chow

*Semiconductor Materials and Device Science Department,  
Sandia National Laboratories, Albuquerque, NM 87185-0601*

S. W. Koch

*Physics Department, Philipps University, Renthof 5, 35037 Marburg, Germany*

A quantum kinetic theory is used to compute excitation induced dephasing in semiconductor quantum dots due to the Coulomb interaction with a continuum of states, such as a quantum well or a wetting layer. It is shown that a frequency dependent broadening together with nonlinear resonance shifts are needed for a microscopic explanation of the excitation induced dephasing in such a system, and that excitation induced dephasing for a quantum-dot excitonic resonance is different from quantum-well and bulk excitons.

PACS numbers: 78.67Hc, 71.35.Cc

Semiconductor quantum dots (QDs) are widely studied, e.g. for quantum optical applications, [1, 2] quantum information processing, [3] or semiconductor laser systems. [4, 5] In all these optical investigations, the excitation induced decoherence of the material polarization driven by optical fields plays a decisive role. The dephasing of the optical polarization limits all externally controllable coherent and quantum entanglement processes, and determines the homogeneous broadening of quantum-dot laser active media. [6, 7, 8] Measurements of polarization dephasing in self-organized QDs have recently been reported, [9] and excitation induced dephasing processes have been observed in interface QDs, where they were found to be important even at low temperatures and densities. [10]

Currently missing is a consistent microscopic theory for the excitation induced dephasing of polarizations created between in QD states due to Coulomb interaction with carriers in continuum states. The traditional analysis of scattering and dephasing processes in condensed matter systems with continuous energy spectra invokes a Markovian approximation, in which the full time-dependence of the dephasing process is neglected and replaced by an instantaneous scattering event. The Markov approximation thus discards the memory time of a scattering process, which corresponds to a quantum-mechanical energy-time uncertainty, and describes dephasing by equations of Boltzmann type using *energy conserving transitions* between quasi-particle states. The continuous energy spectra of carriers in bands ensure that through the energy-momentum relation in two or three dimensions a large phase space contributes to the scattering/dephasing processes. Moreover, scattering/dephasing processes for a continuum of states do not single out one energy because the relevant physical quantities are obtained by an average over a range of energies.

For the dephasing of the optical polarization in QD structures such a treatment needs to be investigated because a discrete QD state enters the energy conservation condition, which reduces the available phase space by restricting the allowed scattering possibilities. [11, 12] Disregarding inhomogeneous broadening, the dephasing affects only the very narrow QD resonance, whose value is *excitation dependent*. Thus one has to take the frequency dependence of the dephasing and the excitation-induced renormalization of the QD resonances seriously. This is done in this paper using a quantum kinetic analysis that avoids the Markovian approximation and thus includes the memory of the interaction with carriers in scattering states leading to polarization dephasing. [13] Another interesting aspect is that the arguments made above against employing the Markov approximation for a narrow resonance also pertains to excitons, i.e., Coulomb bound states. The non-Markovian calculation treats both types of bound states (QD resonances and excitons) on an equal footing and the different behavior of the two types of bound states can be investigated.

In this letter we present a microscopic non-Markovian calculation of the excitation induced polarization dephasing for a model representing shallow epitaxially grown or interface QDs. The heterostructure is treated as a system of QDs embedded in a quantum well (QW) and the optical polarization is computed including the Coulomb interaction between carriers in the dot states and carriers populating the continuum of scattering states in the QW. The Coulomb interaction causes excitation dependent modifications of QD optical response to external fields: First, the non-Markovian treatment of the Coulomb interaction between QDs and surrounding QW leads to an energy dependence of the polarization dephasing. Second, excitation-induced shifts of the QD resonance energies are obtained, in agreement

with experimental results. It is shown that the combination of resonance-shifts and energy dependent polarization dephasing leads to an excitation dependence of the QD optical response that is qualitatively different from the QW and bulk systems.

Our analysis starts from the standard many-particle Hamiltonian including Coulomb interacting electrons and holes with dipole coupling to a classical electromagnetic field. [14] Since we are modelling QD and QW states interacting via the Coulomb potential, [15] the relevant Coulomb interaction energy matrix element  $V_{rsnm} = \sum_{\vec{q} \neq 0} V_q I_{nm}(q)^* I_{rs}(q)$  contains the Fourier-transformed QW Coulomb potential  $V_q$  and overlap integrals  $I_{rs}(q) = \int d^2r \phi_r^*(r) e^{-i\vec{q}\cdot\vec{r}} \phi_s(r)$ . Here  $\phi_n(r)$  is a carrier envelope function in the plane of the QW, which can be localized or delocalized, describing a dot or wetting layer state, respectively. The integral is extended over the QW plane. We neglect the interaction with phonons because this interaction mechanism gives an excitation-independent background dephasing that can be separated from the excitation-induced contribution. [9]

We apply the nonequilibrium Green's functions technique [16, 17] to compute the linear optical response using the free generalized Kadanoff-Baym ansatz according to the general approach presented in Ref. [18, 19]. In order to illustrate the physical effects due to the interaction between carriers in QD and QW states, we treat the case of one localized state (denoted by "0" for the QD ground state) that is coupled to delocalized scattering states (denoted by  $k$  for the wetting layer or QW states) for electrons and holes. Typically, in realistic systems different QDs are sufficiently far apart that there is no coupling between dots at different positions. We furthermore assume identical single-particle wave functions for electrons and holes to avoid the distortion of the continuum states due to charged dots. Then the dynamical variables are the polarizations of the QD,  $p_0 = \langle b_0 a_0 \rangle$ , and the QW,  $p_k = \langle b_k a_k \rangle$ . For the evaluation of the probe absorption spectra, we retain all terms linear in the induced probe polarization to obtain dynamical equations for  $p_0$  and  $p_k$ , in which the dephasing is described by memory integrals over interaction processes with the continuum. We do not employ a Markov approximation and transform the dynamical equations to frequency space. The resulting Fourier-transformed polarization equations with energy dependent scattering rates contain the full memory of the polarization dynamics in the time domain.

In detail, the electron-hole polarization connecting the electron and hole ground states ("0") is determined by

$$(\hbar\omega - \epsilon_{0,\text{HF}}^e - \epsilon_{0,\text{HF}}^h)p_0 + \hbar\Omega_{00,\text{HF}}(1 - n_0^e - n_0^h) = iS_0(\omega) \quad (1)$$

with the scattering contribution

$$S_0(\omega) = -\Lambda_{00}p_0(\omega) + \sum_{\vec{k}'} \Lambda_{0,k'}p_{k'}(\omega). \quad (2)$$

In Eq. (1), the Rabi energy  $\hbar\Omega_{00,\text{HF}}$  and the QD single-particle energies  $\epsilon_{0,\text{HF}}^\alpha$  ( $\alpha = e, h$ ) are renormalized energies containing the many-body Hartree-Fock contributions, and the bare QD energies  $\epsilon_0^\alpha$  contain the QD electron-hole binding energy. The carrier distribution functions are denoted by  $n_0^\alpha$ . The Hartree-Fock contributions to  $\hbar\Omega_{00,\text{HF}}$  and  $\epsilon_{0,\text{HF}}^\alpha$  are linear in the bare Coulomb potential, [14] whereas the correlation (or scattering) contributions  $S_0(\omega)$  are given in 2nd Born approximation. [19] Since we assume a quasi-equilibrium situation with temporally constant electron and hole populations, we can analytically evaluate the Fourier transform of the non-Markovian dynamical equation for the scattering contributions that determine the optical response to the weak probe pulse. The result for the frequency dependent diagonal part is

$$\begin{aligned} \Lambda_{00}(\omega) = & \frac{1}{A^2} \sum_{\vec{q} \neq 0, \vec{k}', \vec{k}''} \sum_{\alpha, \beta = e, h} g(\hbar\omega - \epsilon_0^\alpha - \epsilon_{k'}^\alpha + \epsilon_{k''+q}^\beta - \epsilon_{k''}^\beta) \\ & [2W_q^2 |I_{0k'}(q)|^2 - \delta_{\alpha\beta} W_q W_{k''-k'+q} I_{0k'}(q) I_{0k''}(k'' - k' + q)^*] \\ & \left[ (1 - n_{k'}^\alpha) n_{k''+q}^\beta (1 - n_{k''}^\beta) + n_{k'}^\alpha (1 - n_{k''+q}^\beta) n_{k''}^\beta \right] \end{aligned} \quad (3)$$

and correspondingly for the off-diagonal parts  $\Lambda_{0,k'}$ , which can be obtained from Eq. (3) by pulling the  $k'$  sum out, making the replacements  $n_{k'}^\alpha \rightarrow n_0^\alpha$  and using  $g(\hbar\omega - \epsilon_0^\alpha - \epsilon_{k'}^\alpha + \epsilon_{k''+q}^\beta - \epsilon_{k''}^\beta)$ . Here,  $g(\epsilon) = \lim_{\eta \rightarrow 0} \frac{i}{\epsilon + i\eta} = \pi\delta(\epsilon) + iP_\epsilon^1$  where  $\epsilon$  is the energy argument and  $P$  denotes the principal part. Furthermore, writing  $\Lambda_{00} = \Gamma_{00} - i\Delta_{00}$ ,  $\Gamma_{00}$  is the dephasing contribution, and  $\Delta_{00}$  the energy renormalization by the correlation contribution that is added to the Hartree-Fock contribution. The screened potential is denoted by  $W_q = V_q/\epsilon_q$ , where  $\epsilon_q$  is the Lindhard dielectric function in static approximation computed using the QW carrier distributions, and the normalization area is denoted by  $A$ . The Markovian limit of Eq. (3) is obtained by using  $g(\epsilon_0^\alpha - \epsilon_{k'}^\alpha + \epsilon_{k''+q}^\beta - \epsilon_{k''}^\beta)$ , which makes  $\Lambda$  frequency independent. For the QW polarizations  $p_k$  the equivalent to  $\Lambda_{00}(\omega)$  is  $\Lambda_{kk}(\omega)$ , which is computed by using

$g(\hbar\omega - \epsilon_k^{\bar{\alpha}} - \epsilon_{k'}^{\alpha} + \epsilon_{k''+q}^{\beta} - \epsilon_{k''}^{\beta})$  and replacing  $I_{0k'}(q) \rightarrow I_{kk'}(q) = \delta(k - k' + q)$ . Thus, the form of Eq. (3) describes the dephasing for both QD and QW states. We choose a parabolic in-plane confinement potential for the QD and a QW width of  $w = 4$  nm, with material parameters typical of the InGaAs/GaAs system. For the scattering states, we use orthogonalized plane waves for the overlap integrals. Equations (1)–(3) couple to the microscopic QW polarizations  $p_k$ . In deriving the equations of motion for the  $p_k$ , we have ignored the influence of the QDs on the QW states since this influence is small for the low QD concentrations considered in the following. The probe absorption spectra are calculated as in Ref. [15].

Figure 1 shows absorption spectra obtained by evaluating Eqs. (1)–(3) and their counterparts for the QW polarizations  $p_k$  for different carrier densities under room-temperature ( $T = 300\text{K}$ ) quasi-equilibrium conditions. Each spectrum exhibits the QD resonance and the absorption due to the extended QW states including the QW excitonic resonance. With increasing carrier density, the bleaching of the QD resonance is accompanied by a pronounced red shift and excitation induced broadening. In contrast, the QW excitonic resonance exhibits only bleaching and broadening, but no energy shift. Such a red shift of the QD ground-state resonance has been observed recently in photoluminescence experiments. [20]

Figure 2 focuses on the line shape of the QD absorption (solid line). Comparison with a Lorentzian least-squares fit curve (dotted line) shows that the linewidth of the QD absorption computed including memory effects is significantly different from a Lorentzian line. Earlier calculations without memory effects, i.e., essentially *Markovian* versions of our approach, have also shown non-Lorentzian excitonic line shapes for bulk and QWs, [14, 19] but the important point here is that the absorption linewidth in *non*-Markovian calculation is smaller than the Markovian result (dashed line). This is surprising because non-Markovian calculations are known to *broaden* yield *broader* spectral features than Markovian treatments because scattering and dephasing are increased compared to the Markovian treatment by including the memory of the interaction processes. [21]

Figure 3 explains why the *non*-Markovian calculation can lead to a smaller dephasing than the Markovian calculation. It shows the real part of Eq. (3), which determines the dephasing, i.e., the broadening of the absorption spectrum. The  $\omega$  dependence of  $\Gamma = \text{Re}\Lambda_{00}$  shows that the non-Markovian calculation does not yield energy conservation among the single-particle states connected by the scattering process, but introduces an additional  $\hbar\omega$  contribution. The non-Markovian calculation can therefore lead to a larger dephasing, but in the present case this is only true for  $\hbar\omega \geq \epsilon_0$  because in this region more QW states can satisfy the argument of the  $\delta$  function, which occurs in the real part of Eq. (3). For energies smaller than the unexcited dot resonance  $\hbar\omega \leq \epsilon_0$ , the opposite effect occurs because less QW energies in Eq. (3) satisfy the argument of the  $\delta$  function. Thus, the QD dephasing is determined the value of  $\Gamma(\omega)$  *at the QD resonance*. As can be seen in Fig. 1 the QD resonance undergoes a redshift and “picks” the dephasing at the energies marked by dots in Fig. 2. The excitation induced shift of the QD resonance is the reason why the non-Markovian calculation leads to a narrower line than the Markovian calculation.

Figure 4 summarizes the results for the excitation dependence of the dephasing. Plotted is the full width at half maximum (FWHM) versus carrier density. The main figure shows the difference between the full (solid curve) and Markovian (dashed curve) calculations. While both curves exhibit a linear dependence of spectral width on carrier density, using the Markovian approximation overestimates both the magnitude and the carrier density dependence. As explained above, this result is a consequence of the frequency dependent effective dephasing rate and the excitation induced red shift of the dot resonance. The inset compares these results to the QW broadening. In addition to an appreciably larger broadening because of a larger phase space that contributes to the scattering integral, the QW spectral width has a superlinear dependence on carrier density, because the QW exciton experiences the excitation induced dephasing at the same energy without counteracting this trend by undergoing a red shift like the QD resonance. Comparison with experiment is best done in terms of the change in spectral width with carrier density, as it eliminates the background due to carrier-phonon scattering. We extracted values of  $3$  to  $6 \times 10^{-18}$  meV/cm $^{-3}$  from single QD measurements, [20] where the variation arises from dot-to-dot fluctuations and uncertainty in carrier density. This range of values compares favorably with our prediction of  $2 \times 10^{-18}$  meV/cm $^{-3}$  (slope of solid curve in Fig. 4), where we used the QW width of 4 nm and assumed  $\epsilon_R = 4$  meV.

In conclusion, we present a non-Markovian quantum-kinetic analysis of the excitation dependent energy renormalization and broadening of QD states that are electronically coupled to a continuum of states, which we model as a QW. The dot resonance displays a density-dependent red shift, which is the counterpart of the band-gap shift for the QW states, whereas the QW excitonic resonance is stationary due to the compensation of gap shift and reduction of the exciton binding energy. The non-Markovian calculation introduces a frequency dependent damping, and its value at the excitation dependent QD resonance determines the magnitude of the polarization dephasing, i.e., the linewidth of the QD resonance. The QD resonance shows a pronounced excitation induced dephasing, but the excitation induced shift of the resonance counteracts the overall increase of the damping to some extent. Compared to the QD resonance, the QW exciton’s damping is larger due to a larger phase space available for the scattering processes, and

its stationary resonance experiences the excitation induced increase of the damping at the QW excitonic resonance and thus a larger excitation induced dephasing.

We thank W. Hoyer, M. Kira, and F. Jahnke for helpful discussions. This work was funded in part by the United States Department of Energy under contract DE-AC04-94AL85000. WWC was supported in part by the Senior Scientist Program of the Humboldt Foundation. SWK thanks the Deutsche Forschungsgemeinschaft, the Humboldt Foundation and the Max-Planck Society for support.

- 
- [1] P. Michler, A. Imamoglu, M. D. Mason, P. J. Carson, G. F. Strouse, and S. K. Buratto, *Nature* **406**, 968 (2000).
  - [2] M. Bayer, T. L. Reinecke, F. Weidner, A. Larionov, A. McDonald, and A. Forchel, *Phys. Rev. Lett.* **86**, 3168 (2001).
  - [3] X. Q. Li, Y. W. Wu, D. Steel, D. Gammon, T. H. Stievater, D. S. Katzer, D. Park, C. Piermarocchi, and L. J. Sham, *Science* **301**, 809 (2003).
  - [4] M. Sugawara, *Self-Assembled InGaAs/GaAs Quantum Dots* (Academic, San Diego, 1999).
  - [5] D. Bimberg, M. Grundmann, and N. N. Ledentsov, *Quantum Dot Heterostructures* (Wiley, New York, 1999).
  - [6] A. V. Uskov, A. P. Jauho, B. Tromborg, J. Mork, and R. Lang, *Phys. Rev. Lett.* **85**, 1516 (2000).
  - [7] H. C. Schneider, W. W. Chow, and S. W. Koch, *Phys. Rev. B* **66**, 041310 (2002).
  - [8] M. Sugawara, K. Mukai, Y. Nakata, H. Ishikawa, and A. Sakamoto, *Phys. Rev. B* **61**, 7595 (2000).
  - [9] P. Borri, W. Langbein, S. Schneider, U. Woggon, R. L. Sellin, D. Ouyang, and D. Bimberg, *Phys. Rev. Lett.* **87**, 157401 (2001).
  - [10] T. Guenther, C. Lienau, T. Elsaesser, M. Glanemann, V. M. Axt, T. Kuhn, S. Eshlaghi, and A. D. Wieck, *Phys. Rev. Lett.* **89**, 057401 (2002).
  - [11] Y. Toda, O. Moriwaki, M. Nishioka, and Y. Arakawa, *Phys. Rev. Lett.* **82**, 4114 (1999).
  - [12] J. Urayama, T. B. Norris, J. Singh, and P. Bhattacharya, *Phys. Rev. Lett.* **86**, 4930 (2001).
  - [13] L. Banyai, D. B. Tran Thoai, E. Reitsamer, H. Haug, D. Steinbach, M. U. Wehner, M. Wegener, T. Marschner, and W. Stolz, *Phys. Rev. Lett.* **75**, 2188 (1995).
  - [14] H. Haug and S. W. Koch, *Quantum Theory of the Optical and Electronic Properties of Semiconductors* (World Scientific, Singapore, 2004).
  - [15] H. C. Schneider, W. W. Chow, and S. W. Koch, *Phys. Rev. B* **64**, 115315 (2001).
  - [16] W. Schäfer and M. Wegener, *Semiconductor Optics and Transport Phenomena* (Springer, 2002).
  - [17] H. Haug and A.-P. Jauho, *Quantum Kinetics in Transport and Optics of Semiconductors*, vol. 123 of *Springer Series in Solid-State Sciences* (Springer, Berlin, 1996).
  - [18] R. Binder and S. W. Koch, *Progress Quant. Electronics* **19**, 307 (1995).
  - [19] G. Khitrova, H. M. Gibbs, F. Jahnke, M. Kira, and S. W. Koch, *Rev. Mod. Phys.* **71**, 1591 (1999).
  - [20] K. Matsuda, K. Ikeda, T. Saiki, H. Saito, and K. Nishi, *Appl. Phys. Lett.* **83**, 2250 (2003).
  - [21] M. Betz, G. Goger, A. Laubereau, P. Gartner, L. Banyai, H. Haug, K. Ortner, C. R. Becker, and A. Leitenstorfer, *Phys. Rev. Lett.* **86**, 4684 (2001).

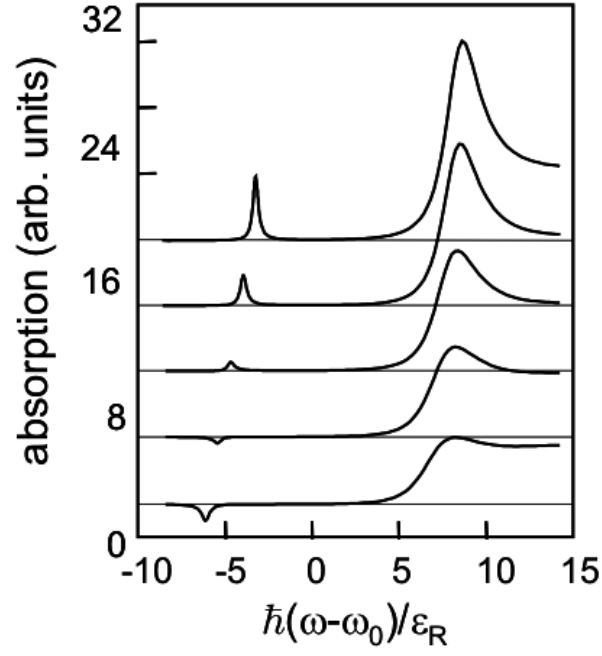


FIG. 1: Room-temperature absorption spectra for the combined quantum-dot/quantum-well system for carrier densities 2 to  $4 \times 10^{11} \text{ cm}^{-2}$  in intervals of  $5 \times 10^{10} \text{ cm}^{-2}$  (top to bottom, the base line of the spectra is shifted). The energy unit is the 3-dimensional exciton binding energy  $\epsilon_R$ , and the zero is at the bare quantum-dot excitonic transition  $\hbar\omega_0$ .

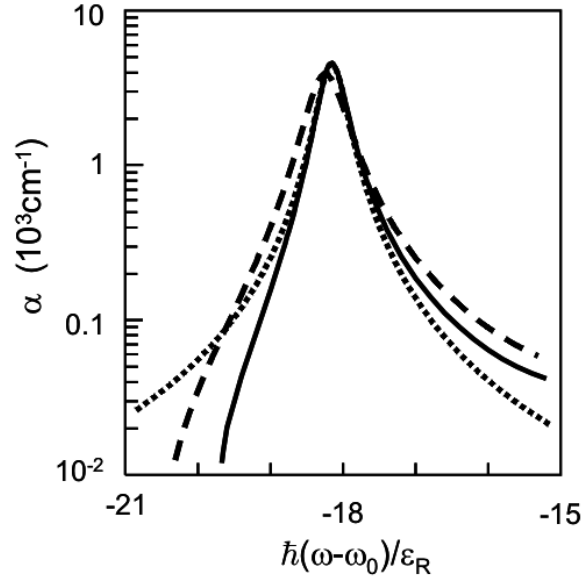


FIG. 2: Absorption spectrum around quantum-dot resonance for carrier density  $2.5 \times 10^{11} \text{ cm}^{-2}$  calculated using the full non-Markovian scattering contributions (solid curve), and the Markov approximation (dashed curve). The dotted curve is obtained from a least-squares fit with a Lorentzian.

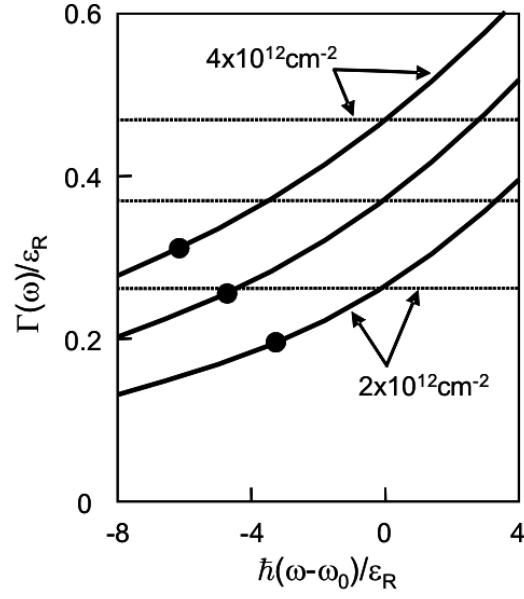


FIG. 3:  $\Gamma(\omega) = \text{Re} \Lambda_{00}(\omega)$  [Eq. (3)] for three different carrier densities. The respective renormalized quantum-dot resonance is marked by a dot.

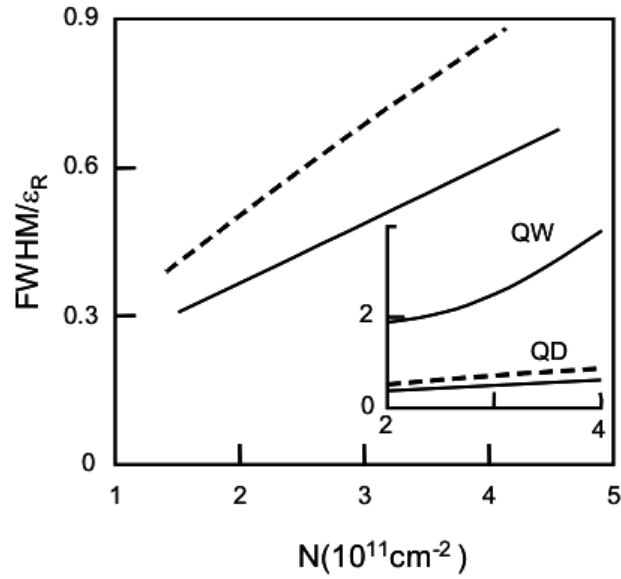


FIG. 4: Excitation dependent broadening of the quantum-dot and quantum-well resonance lines calculated using the full non-Markovian scattering contributions (solid lines) and the Markov approximation (dashed line). Inset: Comparison to excitation induced broadening of the quantum-well excitonic resonance. The energy unit is the 3-d exciton binding energy.